THE JOURNAL OF PHYSICAL CHEMISTRY C

Article

pubs.acs.org/JPCC

Optical Origin of Subnanometer Resolution in Tip-Enhanced Raman Mapping

Chao Zhang, Bao-Qin Chen, and Zhi-Yuan Li*

Laboratory of Optical Physics, Institute of Physics, Chinese Academy of Sciences, P.O. Box 603, Beijing 100190, China

ABSTRACT: Raman spectroscopy and imaging at the single-molecular level in both signal sensitivity and spatial resolution have been a long dream. A recent experimental study of single-molecule Raman mapping with a subnanometer resolution by using a tip-enhanced Raman scattering (TERS) technique is a great step closer to this great dream. However, how the subnanometer spatial resolution is possible with a Raman excitation light spot ("hot spot") of diameter over 10 nm formed between the tip−substrate nanogap to excite and probe the molecule still remains mysterious. Here we present an optical theory of Raman scattering that accounts for the strong near-field self-interaction of molecule with the plasmonic nanogap due to multiple elastic scattering of light by the molecule. The result shows that the self-interaction effect strongly modulates the Raman excitation and radiation in both the signal intensity and spatial sensitivity, leading to a "super-hot spot" and subnanometer lateral resolution of Raman mapping. The optical theory can help to uncover the full picture of light-matter interaction of atoms and molecules with plasmonic nanostructures and explore unknown frontiers of physics and chemistry at nanoscale.

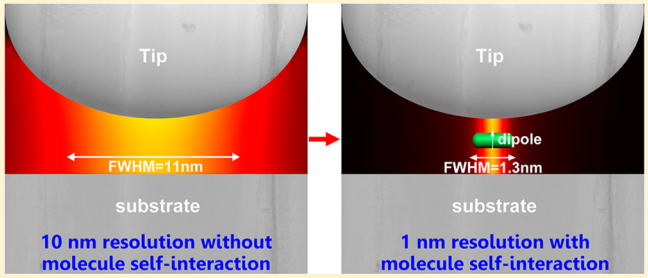

I. INTRODUCTION

Raman spectroscopy offers a powerful means to observe vibrational, rotational, and other low-frequency modes in molecules, and has become a popular and useful technology for molecular identification. A fundamental dream of Raman spectroscopic science and technology is to probe Raman signal with ultrahigh spectroscopic sensitivity down to single-molecule detection level and ultrahigh spatial resolution down to the single-molecule size scale. This would allow people to identify, monitor, and manipulate single molecules both in temporal and spatial domain. As the cross section of Raman scattering is extremely low under usual conditions of laser excitation, many methods have been explored to advance the power of Raman spectroscopy to the fundamental single-molecule limit. Among them, surface plasmon resonance (SPR) effect in metallic nanostructures has been a promising means.[1−11] SPR would allow giant enhancement of the interaction between laser and molecules adsorbed in specially designed and prepared metallic nanostructures under the scheme of surface-enhanced Raman spectroscopy (SERS) to the level of single-molecule detection limit.[4,5]

When Raman spectroscopy works together with various mature scanning probe microscopy technologies under the scheme of tip-enhanced Raman spectroscopy (TERS), the spatial resolution of Raman probing and monitoring can be greatly upgraded to a level far below the diffraction-limit scale (about half the laser wavelength, usually several hundred nanometers).[6−15] The metal tip in either atomic force microscopy (AFM) or scanning tunneling microscopy (STM) can induce a highly concentrated electric field focus spot with greatly enhanced field intensity in the vicinity of the tip apex due to SPR effect. In addition to Raman scattering, the SPR effect can enhance many other physical processes, such as fluorescence,[16−20] catalysis,[21−23] nonlinear optics[24] and other interactions.[25−27] The focus spot, with a size as small as 10 nm, will excite molecules significantly only within its landscape. As a result, both high-sensitivity and high spatial resolution of Raman spectroscopy can be achieved by TERS.[6−10] Although many methods like coherent anti-Stokes Raman scattering,[13] chemical[14,15] and physical contact[9] have been used to improve the spatial resolution and other performances of TERS, the ultrahigh vacuum (UHV) TERS[8,10,11,15] provides a general and reliable system to have high spatial resolution for many molecules.

It is generally believed that the spatial resolution of TERS is nearly the same as the focus spot size of the metallic AFM or STM tip, which strongly depends on many factors, such as the molecule-tip vertical distance, the curvature radius of tip, the excitation wavelength, and the substrate composition, but at best is in the order of 10 nm. Therefore, it is generally expected that the purely optical Raman signal probe can only achieve a spatial resolution in the order of 10 nm, which is far away from a single-molecule criterion (~1 nm), although both AFM and STM can map the surface tomography of microscopic objects at the subangstrom resolution level. The situation is similar to the conventional optical microscope, where the resolution is the same as the focus spot size of light formed by the objective lens and subject to the Rayleigh diffraction limit of light.

Received: March 19, 2015
Revised: April 27, 2015
Published: April 30, 2015

DOI: 10.1021/acs.jpcc.5b02653
J. Phys. Chem. C 2015, 119, 11858−11871

Recently, this general rule of wisdom has been broken down in a recent work by Dong and co-workers.[11] The team has built a TERS system based on sophisticated ultrahigh vacuum and low temperature STM technologies as well as adopting a double-resonance enhancement scheme for both Raman excitation and emission. Although the size of hot spot around the STM tip is still in the order of 10 nm, the team has been able to achieve an ultrahigh spatial resolution of Raman spectroscopy sufficient for chemical mapping of the subnanometer interior details of a single H2TBPP organic molecule adsorbed on the Ag(111) surface. This beautiful experiment has opened a new window to perform chemical imaging at the single-molecule level. Nonetheless, the physical mechanism underlying this surprising experimental observation is still unclear. Obviously there is a huge gap between the conventional wisdom (~10 nm) and the experimental observation (~1 nm) in regard to the spatial resolution of Raman mapping. What can act as the bridge to connect this 1 order of magnitude huge gap? In this work we offer a solution to this puzzling problem. We will show that the strong near-field self-interaction of the molecule with the plasmonic nanogap in the TERS system will make the molecule itself an indispensable part of the strongly correlated tip-molecule−substrate nanosystem and significantly enhance both the signal intensity and spatial resolution of Raman mapping.

The paper is organized as follows. In section II, we present a brief introduction to the conventional theory for plasmon enhanced Raman scattering. In section III, we use the conventional theory to calculate the spatial resolution of TERS system in ref 11, and find that the old theory yields a spatial resolution far larger than the experimental observation. In section IV, we derive a new theory for Raman enhancement considering molecule self-interaction. In section V, we use our theory to calculate the spatial resolution of TERS system and find that the new theory yields a subnanometer spatial resolution that agrees with the experimental observation. In section VI, we make an estimate of near-field self-interaction contribution to Raman enhancement. Finally, in section VII, we summarize this paper and make our conclusions.

II. CONVENTIONAL THEORY FOR PLASMON-ENHANCED RAMAN SCATTERING

Raman scattering involves interaction of optical field with quantum states of Raman molecules. Therefore, the enhancement of Raman signal contributes from the electromagnetic factor and the chemical factor. The electromagnetic enhancement factor is closely related with the local electric field enhancement. According to the traditional surface enhanced Raman scattering (SERS) and tip-enhanced Raman scattering (TERS) theory, the intensity of spontaneous Raman radiation is nearly proportional to the fourth power of the local filed enhancement and linear to the excitation intensity I_0.[1,2] Although that is an approximate result, it always shows good agreement with experiment for general situations. Some more accurate calculations for the enhancement factor of SERS that are based on optical reciprocity theorem and specific experimental conditions have been made,[28] and some more accurate definition for single molecule SERS enhancement factor has also been discussed.[29] In the scalar phenomenological theory[12] that we adopt in the current work, the Raman enhancement could owe to the separate contribution from the excitation and radiation enhancement process. In the dipole approximation the Stokes (anti-Stokes) light radiated by the vibration molecule could be expressed as the radiation by the induced dipole $\boldsymbol{\mu}(\omega_R)$. In the plasmonic nanostructure environment, $\boldsymbol{\mu}(\omega_R)$ is given by

$$\begin{aligned}\boldsymbol{\mu}(\omega_R) &= \alpha(\omega_R, \omega)\mathbf{E}(\mathbf{r}_0, \omega)\\ &= \alpha(\omega_R, \omega)[\mathbf{E}_0(\mathbf{r}_0, \omega) + \mathbf{E}_s(\mathbf{r}_0, \omega)]\end{aligned} \tag{2.1}$$

where ω is the frequency of excitation radiation, ω_R is the Stokes (anti-Stokes) frequency of Raman signal, and $\boldsymbol{r}_0$ is the molecule's site. The polarizability $\alpha(\omega_R, \omega)$ (called Raman tensor in general) describes the transition intensity of Raman frequency shift process that connects the excitation frequency and the vibration shift frequency, and it is closely related with the molecular quantum states involved with the Raman process. The local field $\boldsymbol{E}(\boldsymbol{r}_0, \omega)$ consists of the incident field $\boldsymbol{E}_0(\boldsymbol{r}_0, \omega)$ and the greatly enhanced scattering field $\boldsymbol{E}_s(\boldsymbol{r}_0, \omega)$ from the nanostructure upon the incident field. In usual Raman experiments, the total local field is a linear function of the excitation field. The local field enhancement factor due to plasmonic nanostructures $f_1(\omega)$ is defined by $|\boldsymbol{E}(\boldsymbol{r}_0, \omega)| = f_1(\omega)|\boldsymbol{E}_0(\boldsymbol{r}_0, \omega)|$. For nanostructures with complicated geometric configuration, this local field enhancement factor does not have a simple analytical formulation, but instead must be determined numerically. When the molecule is placed in vacuum and is excited by $\boldsymbol{E}(\boldsymbol{r}_0, \omega)$, the corresponding dipole moment would be

$$\boldsymbol{\mu}_0(\omega_R) = \alpha(\omega_R, \omega)\mathbf{E}_0(\mathbf{r}_0, \omega) \tag{2.2}$$

Obviously, we have $f_1(\omega) = |\boldsymbol{E}(\boldsymbol{r}_0, \omega)|/|\boldsymbol{E}_0(\boldsymbol{r}_0, \omega)| = |\boldsymbol{\mu}(\omega_R)|/|\boldsymbol{\mu}_0(\omega_R)|$.

The Raman radiation far field from the induced dipole $\boldsymbol{\mu}(\omega_R)$ is given by the following formula

$$\begin{aligned}\mathbf{E}(\mathbf{r}_\infty, \omega_R) &= \frac{\omega_R^2}{\varepsilon_0 c^2}\vec{\mathbf{G}}(\mathbf{r}_\infty, \mathbf{r}_0, \omega_R)\cdot\boldsymbol{\mu}(\omega_R)\\ &= \frac{\omega_R^2}{\varepsilon_0 c^2}[\vec{\mathbf{G}}_0(\mathbf{r}_\infty, \mathbf{r}_0, \omega_R) + \vec{\mathbf{G}}_s(\mathbf{r}_\infty, \mathbf{r}_0, \omega_R)]\cdot\boldsymbol{\mu}(\omega_R)\end{aligned} \tag{2.3}$$

In comparison, the Raman radiation far field by the dipole $\boldsymbol{\mu}(\omega_R)$ placed in vacuum would be simply

$$\mathbf{E}_0(\mathbf{r}_\infty, \omega_R) = \frac{\omega_R^2}{\varepsilon_0 c^2}\vec{\mathbf{G}}_0(\mathbf{r}_\infty, \mathbf{r}_0, \omega_R)\cdot\boldsymbol{\mu}(\omega_R) \tag{2.4}$$

The total Green function $\vec{\mathbf{G}}(\boldsymbol{r}_\infty, \boldsymbol{r}_0, \omega_R)$ (a second rank tensor described by a 3×3 matrix) could split into the free space Green function $\vec{\mathbf{G}}_0(\boldsymbol{r}_\infty, \boldsymbol{r}_0, \omega_R)$ and the scattering Green function $\vec{\mathbf{G}}_s(\boldsymbol{r}_\infty, \boldsymbol{r}_0, \omega_R)$, which describes the influence, in particular, enhancement due to plasmonic nanostructures. We can define another enhancement factor to describe this improvement of the radiation power of a dipole assisted by its plasmonic nanostructure environment, namely, $f_2(\omega_R) = |\boldsymbol{E}(\boldsymbol{r}_\infty, \omega_R)|/|\boldsymbol{E}_0(\boldsymbol{r}_\infty, \omega_R)|$. Notice that the Green function exactly describes the power of a given dipole to radiate its optical energy from near field to far field in a particular electromagnetic environment. According to eqs 2.3 and 2.4, $f_2(\omega_R)$ is equal to the quantity of the total Green function projected to the dipole moment $\boldsymbol{\mu}(\omega_R)$ orientation (unit vector $\mathbf{n}$) over that of the free space Green function, $f_2(\omega_R) = |\vec{\mathbf{G}}(\boldsymbol{r}_\infty, \boldsymbol{r}_0, \omega_R)\cdot\mathbf{n}|/|\vec{\mathbf{G}}_0(\boldsymbol{r}_\infty, \boldsymbol{r}_0, \omega_R)\cdot\mathbf{n}|$, which can be approximated by $f_2(\omega_R) \approx \mathrm{Tr}[\vec{\mathbf{G}}(\boldsymbol{r}_\infty, \boldsymbol{r}_0, \omega_R)]/\mathrm{Tr}[\vec{\mathbf{G}}_0(\boldsymbol{r}_\infty, \boldsymbol{r}_0, \omega_R)]$ when averaging over the dipole orientation. Here Tr[...] means the trace of a matrix. For

DOI: 10.1021/acs.jpcc.5b02653
J. Phys. Chem. C 2015, 119, 11858−11871

nanostructures with complicated geometric configuration, this enhancement factor also must be determined numerically.

Combining eqs 2.1−2.4, the Raman radiation far field of a molecule placed in the plasmonic nanostructure is given by

$$\mathbf{E}(\mathbf{r}_\infty, \omega_R) = \frac{\omega_R^2}{\varepsilon_0 c^2}\alpha(\omega_R, \omega)\vec{\mathbf{G}}(\mathbf{r}_\infty, \mathbf{r}_0, \omega_R)\cdot\mathbf{E}(\mathbf{r}_0, \omega) \tag{2.5}$$

In comparison, the Raman radiation far-field for the molecule placed in vacuum is simply

$$\mathbf{E}_{vac}(\mathbf{r}_\infty, \omega_R) = \frac{\omega_R^2}{\varepsilon_0 c^2}\alpha(\omega_R, \omega)\vec{\mathbf{G}}_0(\mathbf{r}_\infty, \mathbf{r}_0, \omega_R)\cdot\mathbf{E}_0(\mathbf{r}_0, \omega) \tag{2.6}$$

Comparison between eq 2.5 and eq 2.6 yields the Raman radiation power enhancement factor as

$$\begin{aligned} G &= \frac{|I(\mathbf{r}_\infty, \omega_R)|}{|I_{vac}(\mathbf{r}_\infty, \omega_R)|} = \frac{|\mathbf{E}(\mathbf{r}_\infty, \omega_R)|^2}{|\mathbf{E}_{vac}(\mathbf{r}_\infty, \omega_R)|^2} \\ &= \frac{|\vec{\mathbf{G}}(\mathbf{r}_\infty, \mathbf{r}_0, \omega_R)\cdot\mathbf{E}(\mathbf{r}_0, \omega)|^2}{|\vec{\mathbf{G}}_0(\mathbf{r}_\infty, \mathbf{r}_0, \omega_R)\cdot\mathbf{E}_0(\mathbf{r}_0, \omega)|^2} \\ &\approx \frac{|Tr[\vec{\mathbf{G}}(\mathbf{r}_\infty, \mathbf{r}_0, \omega_R)]|^2}{|Tr[\vec{\mathbf{G}}_0(\mathbf{r}_\infty, \mathbf{r}_0, \omega_R)]|^2} \times \frac{|\mathbf{E}(\mathbf{r}_0, \omega)|^2}{|\mathbf{E}_0(\mathbf{r}_0, \omega)|^2} \\ &\approx [f_1(\omega)]^2 \times [f_2(\omega_R)]^2 \\ &= G_E(\omega) \times G_R(\omega_R) \end{aligned} \tag{2.7}$$

where $G_E(\omega)$ and $G_R(\omega_R)$ are the enhancement factor in the Raman excitation and radiation processes, respectively. Combining eq 2.5−2.7 the total enhanced Raman intensity is

$$\begin{aligned} I(\mathbf{r}_\infty, \omega_R) &= [f_1(\omega)]^2[f_2(\omega_R)]^2 \\ &\times \frac{\omega_R^4}{\varepsilon_0^2 c^4}|\alpha(\omega_R, \omega)\vec{\mathbf{G}}_0(\mathbf{r}_\infty, \mathbf{r}_0, \omega_R)\cdot\mathbf{n}|^2 I_0(\mathbf{r}_0, \omega) \end{aligned} \tag{2.8}$$

Here $I_0(r_0, \omega)$ is the intensity of the incident light acting at the Raman molecule.

It has been well-established that plasmonic nanostructures not only can enhance the incident field to a greatly intensified local field via various physical processes like surface plasmon resonance effect or near-field scattering effect, it also can significantly enhance the radiation power of molecular Raman signal from the near field region to the far field region (where the detector is placed) through various physical processes such as surface plasmon resonance effect or optical antenna effect. In fact, the excitation and radiation enhancement is closely connected with each other (almost equal to each other) as they follow the electromagnetic reciprocity principle. Generally speaking, if a nanostructure can enhance accumulation of the far-field incident light to the local field, it can equally enhance the emission of local field to the far-field radiation light. As a result, $f_1(\omega) = |E(r_0, \omega)|/|E_0(r_0, \omega)| \approx |E(r_\infty, \omega_R)|/|E_0(r_\infty, \omega_R)| = f_2(\omega_R)$ due to the small shift of Raman radiation frequency ω_R relative to the excitation frequency ω. In this situation, the overall Raman signal enhancement factor is approximately equal to the fourth power of the local field enhancement factor, namely

$$G(\mathbf{r}_0) = |\mathbf{E}(\mathbf{r}_0, \omega)|^4/|\mathbf{E}_0(\mathbf{r}_0, \omega)|^4 \tag{2.9}$$

This fundamental result of traditional SERS theory has long been the physical basis for describing all SERS and TERS phenomena, including the spatial resolution of Raman mapping.[8−11]

III. CONVENTIONAL THEORY APPLIED TO TERS SYSTEM

The schematic configuration of the TERS system used to point-by-point map the Raman image of a single H2TBPP organic molecule adsorbed on Ag(111) surface is illustrated in Figure 1a. We first use the three-dimensional finite-difference time-domain (3D FDTD) method to simulate the local electric field intensity profile of nanogap plasmonic mode excited by a p-polarized incident plane-wave light. A strong enhancement of electric field is seen clearly in Figure 1b, which corresponds to the existence of a "hot spot" located within the nanogap. The full-width at half-maximum (fwhm) of the plasmonic "hot spot" is about 11 nm, which is substantially larger than the lateral size of the H2TBPP molecule (~2 nm).

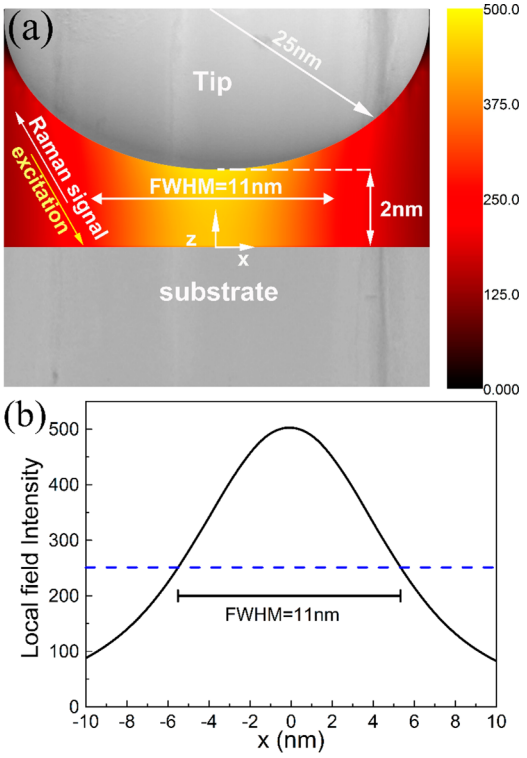

Figure 1. Local electric field profile in the gap region of TERS system calculated by FDTD. (a) The schematic configuration of TERS system used for Raman mapping of molecule. The radius of the tip head is 25 nm, the gap between the tip head with the substrate is 2 nm, the excitation light is at wavelength 532 nm, incidence angle 60°, and *p*-polarization. The intensity profile of local electric field as calculated by 3D FDTD method is displayed within the gap, showing a highly localized "hot spot" centered right below the tip apex. (b) 1D profile of electric field intensity versus the horizontal *x*-axis coordinate at the middle of the gap, where the tip apex is located at $x = 0$ nm. The fwhm of the gap mode "hot spot" is about 11 nm.

According to the conventional plasmon enhanced Raman scattering theory, a molecule located in the vicinity of plasmonic nanostructures will be excited by strongly enhanced local electric field $E(r_0, \omega)$, which has an amplitude enhancement factor $f_1(\omega) = |E(r_0, \omega)|/|E_0(r_0, \omega)|$ over the

DOI: 10.1021/acs.jpcc.5b02653
J. Phys. Chem. C 2015, 119, 11858−11871

incident field $\boldsymbol{E}_0(r_0, \omega)$, and jump from its ground level to higher intermediate quantum states with greatly increased transition probability. Then the molecule subsequently makes spontaneous transitions from these intermediate excited states to lower Stokes or anti-Stokes levels. The emitted photon at frequency ω_R will be scattered away by the plasmonic nanostructures to far-field region with a great enhancement factor defined as $f_2(\omega_R) = |\boldsymbol{E}(r_\infty, \omega_R)|/|\boldsymbol{E}_0(r_\infty, \omega_R)|$, where $\boldsymbol{E}(r_\infty, \omega_R)$ and $\boldsymbol{E}_0(r_\infty, \omega_R)$ are the far-field radiation of molecule (modeled as an electric dipole) with and without the assistance of plasmonic nanostructures. Thus, the Raman enhancement in TERS and SERS involves contribution from excitation enhancement and radiation enhancement. As both factors are approximately equal to the enhancement factor of local field intensity $|\mathbf{E}(\mathbf{r}_0, \omega)|^2/|\mathbf{E}_0(\mathbf{r}_0, \omega)|^2$, altogether the Raman signal enhancement factor is given by

$$G(\mathbf{r}_0) = [f_1(\omega)]^2 \times [f_2(\omega_R)]^2 \approx |\mathbf{E}(\mathbf{r}_0, \omega)|^4/|\mathbf{E}_0(\mathbf{r}_0, \omega)|^4 \tag{3.1}$$

The strong enhancement and tight localization of nanogap plasmonic mode naturally bring even more drastic enhancement of Raman signal. Besides, the Raman signal is highly sensitive to the gap mode profile and decays drastically when leaving the center of the hot spot. Numerical simulation based on eq 3.1 reveals the spatial resolution (defined as the fwhm) of Raman mapping is about 7.2 nm (Figure 4b). This value is much larger than the lateral scale of the H2TBPP molecule. It is thus expected that TERS should not be able to resolve a single H2TBPP molecule, not to say its internal subtle structure such as the central molecular skeleton. Such a prediction made by the conventional Raman scattering theory obviously is at odd with the experimental observation reported in ref 11, which clearly illustrated subnanometer lateral spatial resolution in TERS sufficient to map the internal structure of the H2TBPP molecular skeleton. How to bridge the huge theory-experiment gap in the TERS mapping, which is sub-10 nm versus subnanometer? There must be something critical missing in the conventional Raman scattering theory in application to the current TERS system and the mysterious observation.

IV. THEORY FOR RAMAN ENHANCEMENT CONSIDERING MOLECULE SELF-INTERACTION

Before we go into the details for constructing a new Raman scattering theory that can fully account for the major physics of Raman processes involved in the UHV-TERS system, we stress here (although it is not a naive thing) that the conventional theory for Raman enhancement as discussed in section II only considers the influence of plasmonic nanostructure neighboring or surrounding a molecule upon the incident field (excitation enhancement) and the radiation power of the molecule (radiation enhancement). The molecule itself only serves as a passive probe to sense and apperceive the local field intensity. The counteractive influence of the molecule itself upon the surrounding electric field environment has been completely neglected, perhaps because so far this thing has not been recognized by the SERS and TERS community over the last five decades. We will make a thorough analysis over this brand new unknown territory of Raman scattering physics and chemistry. The result will show that the molecule itself can impose a tremendous counteractive influence over its electromagnetic environment at nanoscale through electromagnetic near-field self-interaction in both the excitation and radiation enhancement processes, and this has a pivotal implication and meaning for the spatial resolution of Raman mapping via a TERS system.

As mentioned above, the molecule has a Raman tensor connecting the excitation light at frequency ω and the Stokes or anti-Stokes scattering light at frequency ω_R. When the molecule size is comparable to the gap size and the distance to the metal surface, its scattering to the light within small gap is so strong that we have to consider the molecule response to the excitation electric field and the Stokes (anti-Stokes) electric field. This is called the electromagnetic self-interaction process of the molecule, which can be characterized as the phenomenological parameter of electric polarizability $\beta(\omega)$ under the dipole approximation, namely $\boldsymbol{p}(r_0, \omega) = \beta(\omega)\mathbf{E}(r_0, \omega)$.

According to the traditional spontaneous Raman enhancement theory described in the last section, we can also attribute the overall contribution upon the modification of molecule polarization to the excitation and radiation process separately. First, in the excitation process the near-field self-interaction of molecule with its environment is characterized by the modification of molecule to the local field. This self-interaction is via the elastic scattering of molecule upon light (either the direct incident light or scattering light) impinging on it. In correspondence to eq 2.1, the new local field could be expressed as

$$\mathbf{E}(\mathbf{r}_0, \omega) = \mathbf{E}_0(\mathbf{r}_0, \omega) + \mathbf{E}_s(\mathbf{r}_0, \omega) + \mathbf{E}_{m,s}(\mathbf{r}_0, \omega) \tag{4.1}$$

where $\boldsymbol{E}_{m,s}(r_0, \omega)$ is the radiation field by the induced dipole $\boldsymbol{p}(r_0, \omega)$ at the excitation wavelength of the molecule. It will be scattered and modified by the surrounding nanostructure and its quantity will be determined self-consistently in a way that will be described later on in this section.

In the radiation process the self-interaction of molecule can also be characterized by the modification to the induced dipole radiating at ω_R. The new radiation filed in the far-field Raman signal detection region could be expressed as

$$\begin{aligned}\mathbf{E}(\mathbf{r}_\infty, \omega_R) &= \frac{\omega_R^2}{\varepsilon_0 c^2}\vec{\mathbf{G}}(\mathbf{r}_\infty, \mathbf{r}_0)\cdot[\boldsymbol{\mu}(\mathbf{r}_0, \omega_R) + \mathbf{p}'(\mathbf{r}_0, \omega_R)] \\ &= \frac{\omega_R^2}{\varepsilon_0 c^2}[\vec{\mathbf{G}}_0(\mathbf{r}_\infty, \mathbf{r}_0) + \vec{\mathbf{G}}_s(\mathbf{r}_\infty, \mathbf{r}_0)]\cdot[\boldsymbol{\mu}(\mathbf{r}_0, \omega_R) + \mathbf{p}'(\mathbf{r}_0, \omega_R)]\end{aligned} \tag{4.2}$$

where $\boldsymbol{p}'(r_0, \omega_R)$ is the modified induced dipole.

As the wavelength of both the excitation and Raman scattering radiation is much larger than the size we care about in the TERS system (including the molecular size, the gap size, and the molecule to substrate and tip surface distances), we can utilize the quasi-electrostatic approximation to describe this near-field self-interaction of molecule with its environment. We could use the method of image in electrostatics to calculate the above modification quantity.[30]

First, $\boldsymbol{E}_{m,s}(r_0, \omega)$ could be considered as the local field generated by a set of image dipoles of the induced dipole $\boldsymbol{p}(r_0, \omega)$ relative to the silver substrate and tip. Simply speaking, the silver substrate influence to the molecule near-field radiation is approximately (but with sufficiently high accuracy) described by the radiation from an image dipole $\boldsymbol{p}_{imag,1}(r_1, \omega)$ located in the image position of r_1, and the silver tip influence to the molecule near-field radiation is approximately (but with sufficiently high accuracy) described by the radiation from another image dipole $\boldsymbol{p}_{imag,2}(r_2, \omega)$ located in the image position

DOI: 10.1021/acs.jpcc.5b02653
J. Phys. Chem. C 2015, 119, 11858−11871

of r_2. The substrate and tip influences to these two secondary image dipoles can be further described by more secondary image dipoles $p_{imag,i}(r_i, \omega)$ located in the image position of r_i. The quantity of these image dipoles, their positions, and their influences can all be calculated analytically.[30] A typical example is depicted in Figure 2.

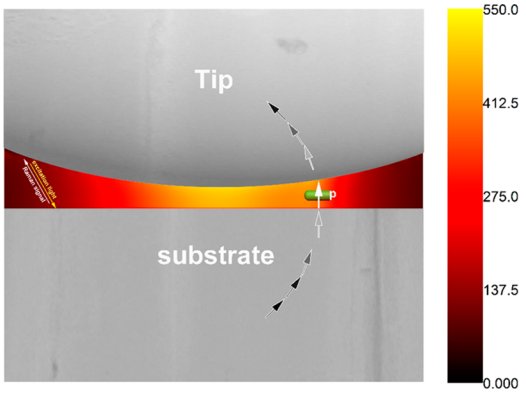

Figure 2. Electromagnetic self-interaction of molecule (modeled as a dipole) within the Ag tip−substrate nanogap. The position and polarization of a series of image dipole are illustrated when the molecule is at 5 nm lateral displacement away from the tip apex and at 1 nm vertical displacement from the substrate. The highly localized "hot spot" around the nanogap is also shown.

Under this image dipole methodology, the overall modified near field could be expressed as

$$\mathbf{E}_{m,s}(\mathbf{r}_0, \omega) = \sum_i \frac{\omega^2}{\varepsilon_0 c^2} \vec{\mathbf{G}}_0(\mathbf{r}_0, \mathbf{r}_i, \omega) \cdot \mathbf{p}_{image,i}(\mathbf{r}_i, \omega) \tag{4.3}$$

where

$$\mathbf{p}_{image,i}(\mathbf{r}_i, \omega) = \vec{\mathbf{M}}_i \cdot \mathbf{p}(\mathbf{r}_0, \omega) \tag{4.4}$$

and $\vec{\mathbf{M}}_i$ are the image matrix that describes the polarization, amplitude and phase change of each image dipole. As has been said above, the overall induced dipole of molecule is proportional to the overall local field, namely

$$\mathbf{p}(\mathbf{r}_0, \omega) = \beta(\omega)\mathbf{E}(\mathbf{r}_0, \omega) \tag{4.5}$$

As the local field and the induced dipole are interrelated, we can use the self-consistent method that has been extensively used in near-filed optics.[31−33] By substituting eqs 4.1, 4.3, and 4.4 into eq 4.5, we can get

$$\mathbf{p}(\mathbf{r}_0, \omega) = \beta(\omega)\left[\mathbf{E}_0(\mathbf{r}_0, \omega) + \mathbf{E}_s(\mathbf{r}_0, \omega) + \sum_i \frac{\omega^2}{\varepsilon_0 c^2} \vec{\mathbf{G}}_0(\mathbf{r}_0, \mathbf{r}_i, \omega)\vec{\mathbf{M}}_i \cdot \mathbf{p}(\mathbf{r}_0, \omega)\right] \tag{4.6}$$

From eq 4.6 we directly find

$$\mathbf{p}(\mathbf{r}_0, \omega) = \beta(\omega)\left[\vec{\mathbf{I}} - \beta(\omega) \sum_i \frac{\omega^2}{\varepsilon_0 c^2} \vec{\mathbf{G}}_0(\mathbf{r}_0, \mathbf{r}_i, \omega)\vec{\mathbf{M}}_i\right]^{-1} \cdot [\mathbf{E}_0(\mathbf{r}_0, \omega) + \mathbf{E}_s(\mathbf{r}_0, \omega)] \tag{4.7}$$

Here $\vec{\mathbf{I}}$ is the unit matrix. According to eq 4.5, the corresponding effective local field is given by

$$\begin{aligned}\mathbf{E}_{N,E}(\mathbf{r}_0, \omega) &= \left[\vec{\mathbf{I}} - \beta(\omega) \sum_i \frac{\omega^2}{\varepsilon_0 c^2} \vec{\mathbf{G}}_0(\mathbf{r}_0, \mathbf{r}_i, \omega)\vec{\mathbf{M}}_i\right]^{-1} \cdot [\mathbf{E}_0(\mathbf{r}_0, \omega) + \mathbf{E}_s(\mathbf{r}_0, \omega)] \\ &= \left[\vec{\mathbf{I}} - \beta(\omega) \sum_i \frac{\omega^2}{\varepsilon_0 c^2} \vec{\mathbf{G}}_0(\mathbf{r}_0, \mathbf{r}_i, \omega)\vec{\mathbf{M}}_i\right]^{-1} \cdot \mathbf{E}(\mathbf{r}_0, \omega)\end{aligned} \tag{4.8}$$

The denotation $[...]^{-1}$ in eqs 4.7 and 4.8 means matrix inversion operation. Comparing eq 4.8 with eq 2.1, the new local field $E_{N,E}$ (r_0, ω) when considering the near-field self-interaction of molecule with its plasmonic environment in the Raman excitation process is now subject to a modification factor over the original local field $E(r_0, \omega)$ without considering this effect. The modification factor is described by the following second rank tensor:

$$\vec{\mathbf{g}}_1(\mathbf{r}_0, \omega) = \left[\vec{\mathbf{I}} - \beta(\omega)\frac{\omega^2}{\varepsilon_0 c^2} \sum_i \vec{\mathbf{G}}_0(\mathbf{r}_0, \mathbf{r}_i, \omega)\vec{\mathbf{M}}_i\right]^{-1} \tag{4.9}$$

Generally the quantity of the modification factor is proportional to the trace of the matrix, which means that the near-field self-interaction modification factor is given by

$$g_1(\mathbf{r}_0, \omega) = |\mathbf{E}_{N,E}(\mathbf{r}_0, \omega)| / \left|\mathbf{E}(\mathbf{r}_0, \omega)\right| \approx \frac{1}{3} Tr[\vec{\mathbf{g}}_1(\mathbf{r}_0, \omega)] \tag{4.10}$$

Now we turn to the Raman radiation process. Following a very similar physical argument and mathematical derivation procedure, we also have

$$\mathbf{p}'(\mathbf{r}_0, \omega_R) = \beta(\omega_R)\mathbf{E}(\mathbf{r}_0, \omega_R) \tag{4.11}$$

According to eq 4.2 the local field at the Raman radiation frequency could be expressed as

$$\begin{aligned}\mathbf{E}(\mathbf{r}_0, \omega_R) &= \frac{\omega_R^2}{\varepsilon_0 c^2} \vec{\mathbf{G}}(\mathbf{r}_0, \mathbf{r}_0, \omega_R) \cdot [\boldsymbol{\mu}(\mathbf{r}_0, \omega_R) + \mathbf{p}'(\mathbf{r}_0, \omega_R)] \\ &= \frac{\omega_R^2}{\varepsilon_0 c^2} \vec{\mathbf{G}}_s(\mathbf{r}_0, \mathbf{r}_0, \omega_R) \cdot [\boldsymbol{\mu}(\mathbf{r}_0, \omega_R) + \mathbf{p}'(\mathbf{r}_0, \omega_R)]\end{aligned} \tag{4.12}$$

The image dipole method under the quasi-electrostatic approximation model can also enable the local field calculation similar to the case of excitation process. We can write directly

DOI: 10.1021/acs.jpcc.5b02653
J. Phys. Chem. C 2015, 119, 11858−11871

$$\vec{\mathbf{G}}_s(\mathbf{r}_0, \mathbf{r}_0, \omega_R)\cdot\mathbf{p}'(\mathbf{r}_0, \omega_R) = \sum_i \vec{\mathbf{G}}_0(\mathbf{r}_0, \mathbf{r}_i, \omega_R)\cdot\mathbf{p}'_{image,i}(\mathbf{r}_i, \omega_R) \tag{4.13}$$

and

$$\mathbf{p}'_{image,i}(\mathbf{r}_i, \omega_R) = \vec{\mathbf{M}}'_i\cdot\mathbf{p}'(\mathbf{r}_0, \omega_R) \tag{4.14}$$

By the self-consistent approach we can get from eqs 4.12−4.14 the following formula

$$\mathbf{p}'(\mathbf{r}_0, \omega_R) = \beta(\omega_R)\frac{\omega_R^2}{\varepsilon_0 c^2}[\vec{\mathbf{G}}_s(\mathbf{r}_0, \mathbf{r}_0, \omega_R)\cdot\boldsymbol{\mu}(\mathbf{r}_0, \omega_R) + \sum_i \vec{\mathbf{G}}_0(\mathbf{r}_0, \mathbf{r}_i, \omega_R)\vec{\mathbf{M}}'_i\cdot\mathbf{p}'(\mathbf{r}_0, \omega_R)] \tag{4.15}$$

which directly yields

$$\begin{aligned}\mathbf{p}'(\mathbf{r}_0, \omega_R) &= \beta(\omega_R)\frac{\omega_R^2}{\varepsilon_0 c^2}\left[\vec{\mathbf{I}} - \beta(\omega_R)\frac{\omega_R^2}{\varepsilon_0 c^2}\sum_i \vec{\mathbf{G}}_0(\mathbf{r}_0, \mathbf{r}_i, \omega_R)\vec{\mathbf{M}}'_i\right]^{-1}\cdot[\vec{\mathbf{G}}_s(\mathbf{r}_0, \mathbf{r}_0, \omega_R)\cdot\boldsymbol{\mu}(\mathbf{r}_0, \omega_R)] \\ &= \beta(\omega_R)\frac{\omega_R^2}{\varepsilon_0 c^2}\left[\vec{\mathbf{I}} - \beta(\omega_R)\frac{\omega_R^2}{\varepsilon_0 c^2}\sum_i \vec{\mathbf{G}}_0(\mathbf{r}_0, \mathbf{r}_i, \omega_R)\vec{\mathbf{M}}'_i\right]^{-1}\cdot[\vec{\mathbf{G}}(\mathbf{r}_0, \mathbf{r}_0, \omega_R)\cdot\boldsymbol{\mu}(\mathbf{r}_0, \omega_R)]\end{aligned} \tag{4.16}$$

According to eq 4.5, the local field related with this induced polarization in the Raman radiation process is

$$\mathbf{E}_{N,R}(\mathbf{r}_0, \omega_R) = \frac{\omega_R^2}{\varepsilon_0 c^2}\left[\vec{\mathbf{I}} - \beta(\omega_R)\frac{\omega_R^2}{\varepsilon_0 c^2}\sum_i \vec{\mathbf{G}}_0(\mathbf{r}_0, \mathbf{r}_i, \omega_R)\vec{\mathbf{M}}'_i\right]^{-1}[\vec{\mathbf{G}}(\mathbf{r}_0, \mathbf{r}_0, \omega_R)\cdot\boldsymbol{\mu}(\mathbf{r}_0, \omega_R)] \tag{4.17}$$

From eq 4.2 we can find that the total induced dipole is

$$\boldsymbol{\mu}_{N,R}(\mathbf{r}_0, \omega_R) = \left[\vec{\mathbf{I}} - \beta(\omega_R)\frac{\omega_R^2}{\varepsilon_0 c^2}\sum_i \vec{\mathbf{G}}_0(\mathbf{r}_0, \mathbf{r}_i, \omega_R)\vec{\mathbf{M}}'_i\right]^{-1}\cdot\boldsymbol{\mu}(\mathbf{r}_0, \omega_R) \tag{4.18}$$

and the far field of Raman radiation is given by

$$\mathbf{E}(\mathbf{r}_\infty, \omega_R) = \frac{\omega_R^2}{\varepsilon_0 c^2}\vec{\mathbf{G}}(\mathbf{r}_\infty, \mathbf{r}_0, \omega_R)\cdot\boldsymbol{\mu}_{N,R}(\mathbf{r}_0, \omega_R) \tag{4.19}$$

Comparing eqs 4.18 and 4.19 with eq 2.3, we can find that there exists a modification factor for the Raman radiation process that originates from the near-field self-interaction of molecule with its plasmonic environment during this Raman radiation process. Similar to the Raman excitation process, this modification factor is also described by the following second rank tensor:

$$\vec{\mathbf{g}}_2(\mathbf{r}_0, \omega_R) = \left[\vec{\mathbf{I}} - \beta(\omega_R)\frac{\omega_R^2}{\varepsilon_0 c^2}\sum_i \vec{\mathbf{G}}_0(\mathbf{r}_0, \mathbf{r}_i, \omega_R)\vec{\mathbf{M}}'_i\right]^{-1} \tag{4.20}$$

The quantity of this modification factor, $g_2(\omega_R)$, which is defined as $g_2(r_0, \omega_R) = |\boldsymbol{\mu}_{N,R}(r_0, \omega_R)|/|\boldsymbol{\mu}(r_0, \omega_R)|$, is also proportional to the trace of the matrix $\vec{\mathbf{g}}_2(\omega_R)$, namely

$$g_2(\mathbf{r}_0, \omega_R) = |\boldsymbol{\mu}_{N,R}(\mathbf{r}_0, \omega_R)|/|\boldsymbol{\mu}(\mathbf{r}_0, \omega_R)| \approx \frac{1}{3}Tr[\vec{\mathbf{g}}_2(\mathbf{r}_0, \omega_R)] \tag{4.21}$$

Taking into account the above analysis of Raman excitation and radiation processes and following the procedure to derive eq 2.7, we can derive the following formula for the modified overall Raman intensity enhancement factor when the near-field self-interaction of the molecule with its electromagnetic environment is fully considered:

$$\begin{aligned}G_S(\mathbf{r}_0) &= \frac{|I(\mathbf{r}_\infty, \omega_R)|}{|I_{vac}(\mathbf{r}_\infty, \omega_R)|} = \frac{|\mathbf{E}(\mathbf{r}_\infty, \omega_R)|^2}{|\mathbf{E}_{vac}(\mathbf{r}_\infty, \omega_R)|^2} \\ &\approx [f_1(\omega)]^2 \times [g_1(\mathbf{r}_0, \omega)]^2 \times [f_2(\omega_R)]^2 \times [g_2(\mathbf{r}_0, \omega_R)]^2 \\ &= G_E(\omega) \times G_{E,S}(\mathbf{r}_0, \omega) \times G_R(\omega_R) \times G_{R,S}(\mathbf{r}_0, \omega_R) \\ &= G(\mathbf{r}_0) \times [G_{E,S}(\mathbf{r}_0, \omega) \times G_{R,S}(\mathbf{r}_0, \omega_R)]\end{aligned} \tag{4.22}$$

For a usual Raman process the shift of Raman radiation frequency ω_R relative to the excitation frequency ω is small. As a result, $g_1(r_0, \omega) \approx g_2(r_0, \omega_R) = g(r_0, \omega)$. In this situation, the modified Raman signal enhancement factor is also approximately equal to the fourth power of the ratio of the modified local field $\mathbf{E}_N(r_0, \omega)$ when considering the near-field self-interaction effect of molecule with respect to the incident field $\mathbf{E}_0(r_0, \omega)$, which is

$$\begin{aligned}G_S(\mathbf{r}_0) &= |\mathbf{E}_N(\mathbf{r}_0, \omega)|^4/|\mathbf{E}_0(\mathbf{r}_0, \omega)|^4 \\ &= g^4(\mathbf{r}_0, \omega)|\mathbf{E}(\mathbf{r}_0, \omega)|^4/|\mathbf{E}_0(\mathbf{r}_0, \omega)|^4\end{aligned} \tag{4.23}$$

In the above, we have adopted a spherical-tip flat-surface model to describe the TERS geometric configuration, from which the near-field self-interaction of the molecule with its environment is calculated analytically by a multiple-image dipole theory. Yet, the concept of near-field self-interaction is applicable to any other geometric configuration in a wide range of plasmon-molecule interaction problems including TERS, SERS, and plasmon enhanced fluorescence. In these cases, the near-field self-interaction of molecules can be written into the following general form

$$\vec{\mathbf{g}}(\mathbf{r}_0, \omega) = [\vec{\mathbf{I}}\text{-}\beta(\omega)\vec{\mathbf{G}}(\mathbf{r}_0, \mathbf{r}_0, \omega)]^{-1} \tag{4.24}$$

DOI: 10.1021/acs.jpcc.5b02653
J. Phys. Chem. C 2015, 119, 11858−11871

where $\overleftrightarrow{\mathbf{G}}(r_0, r_0, \omega)$ represents the near-field self-interaction of the molecule with its environment. The exact form and magnitude of $\overleftrightarrow{\mathbf{G}}(r_0, r_0, \omega)$ usually request extensive numerical simulations.

The above discussions more or less focus on the mathematical formalism of the new Raman scattering theory associated with the UHV-TERS system. In the following we further present a more comprehensive discussion on the physical mechanism involved in the molecular self-interaction in TERS, with a hope to offer an easy-to-understand general physical picture about the puzzling problem of subnanometer resolution in Raman mapping. As is well-known, light-matter interaction in plasmonic nanostructures involves two aspects. On the one hand, many plasmonic nanostructures, such as nanoantenna and nanogap could generate huge field enhancement and large photon density of states to have large impact on matter, for instance, greatly enhance Raman, fluorescence, nonlinear optical and other types of light-matter interaction. On the other hand, matter could counteract and have impact on the optical field in plasmonic nanostructures. For example, the SPR effect is sensitive to the tiny refractive index change of surrounding environment, leading to prominent effects like shift in the SPR peak, which could be used to build highly sensitive biochemical sensors.[34,35] Careful analysis indicates that both aspects of light-matter interaction are present in the TERS system under study and could play a critical role in achieving huge Raman scattering enhancement and high spatial resolution simultaneously. Thus, it is necessary to consider the complicated near-field self-interaction of molecules with its plasmonic nanostructure environment.

In our new theory, there exist two modification factors induced by the near-field self-interaction of the molecule with its plasmonic environment, one to the local field in the Raman excitation process, and the other to the radiation dipole moment in the Raman radiation process. For the sake of clarity and convenience of imagination and thinking about the physics, we schematically illustrate in Figure 3 the major physical picture involved in the conventional Raman scattering theory and our new Raman scattering theory. The similarity and difference of the two theories can be seen clearly: eq 4.23 with eq 3.1 shows that the new theory adds a supplemental term equal to the fourth power of the near-field self-interaction modification factor to the conventional Raman enhancement factor. A plenty of new physics are involved in this theory. In the traditional Raman scattering theory, the molecule is purely passive in both the excitation and radiation processes as it does not change the properties of its plasmonic environment. In contrast, in the new theory, the molecule not only probes the local electric field shaped by its plasmonic environment in both the excitation and radiation processes, but also change the properties of such a plasmonic environment via elastic scattering so that it is different from a bare environment without the molecule. Besides, such a change will inversely counteract upon and modify the Raman excitation and radiation processes. In some sense, this is a highly nonlinear phenomenon. It will become clear that the effect is dependent on the near-field self-interaction strength, and will bring many new characteristics including the subnanometer spatial resolution of TERS.

V. NEW RAMAN ENHANCEMENT THEORY APPLIED TO TERS SYSTEM

For the UHV-TERS setup used in ref 11, the near-field self-interaction modification factor $g(r_0, \omega)$ is approximately

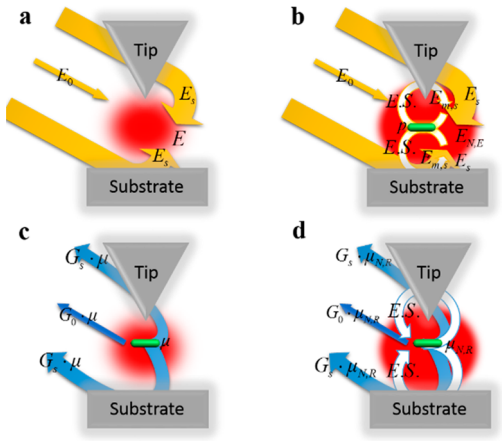

Figure 3. Schematic diagram for normal spontaneous Raman enhancement and molecule self-interaction assisted Raman enhancement. (a) Excitation process of normal spontaneous Raman enhancement, where the incident light is scattered by the Ag tip−substrate gap to form highly localized plasmonic gap mode with greatly enhanced electric field intensity. E_0 and E_s (yellow arrows) are the incident and scattering electric field at frequency ω, summing up to the local field E. (b) Excitation process of spontaneous Raman enhancement when considering the molecule self-interaction with the Ag tip−substrate gap through multiple elastic scattering (white arrows, abbreviated by ***E.S.***) for the incident light. $E_{m,s}$ is the modified excitation field due to the ***E.S.*** mechanism and p is the induced dipole moment describing the molecule response to the excitation light. (c) Radiation process of normal spontaneous Raman enhancement, where the Raman signal at frequency ω_R emitted by the molecule is scattered by the Ag-substrate gap to have greatly enhanced far-field intensity. $G_0\cdot\mu$ and $G_s\cdot\mu$ (blue arrows) are the direct Raman radiation of molecule (described by the dipole moment μ) and greatly enhanced scattering Raman radiation by the tip−substrate gap, where G_0 and G_s are free-space and scattering dyadic Green's function. (d) Radiation process of spontaneous Raman enhancement when considering the molecule self-interaction with the Ag tip−substrate gap through multiple elastic scattering for the Raman radiation signal. The multiple ***E.S.*** mechanism (white arrows) strongly modifies the molecule dipole moment to a value $\mu_{N,R}$.

described by interaction of the molecule dipole with its image dipoles with respect to the flat Ag substrate and the Ag tip, as well as interaction among the image dipoles, reflecting the multiple elastic scattering of molecule radiation within the deep subwavelength nanogap region. Several factors are involved in the UHV-TERS setup to enhance the molecule near-field self-interaction modification factor $g(r_0, \omega)$. First, the H2TBPP organic molecule has a linear size in the order of 1−2 nm so that its polarizability $\beta(\omega)$ is on a sufficiently large level. Second, the Raman radiation of molecule is resonantly excited by light with wavelength matched well with the direct Raman transition band, and this further greatly increases the molecular polarizability $\beta(\omega)$. Third, the width of Ag-substrate Ag-tip nanogap is in the order of several nanometers so that the molecule distance to the nanogap lower and upper surface is both in the order of 1−2 nm and comparable to the molecule size. This makes the near-field dipole−dipole interaction strength $\overleftrightarrow{\mathbf{G}}(r_0, r_0, \omega)$ (inversely proportional to the third power of dipole−dipole distance) to take a high level. Finally, as the molecule is placed within the nanogap, its radiation is subject to an efficient multiple reflection effect and the molecule dipole can interact with all of its image dipoles for many times, which further greatly enhances the near-field self-

DOI: 10.1021/acs.jpcc.5b02653
J. Phys. Chem. C 2015, 119, 11858−11871

interaction strength (namely, dipole-image dipole interaction) described by $\overleftrightarrow{\mathbf{G}}(r_0, r_0, \omega)$. Considering all these factors, the near-field self-interaction term $\beta(\omega)\overleftrightarrow{\mathbf{G}}(r_0, r_0, \omega)$ can have a magnitude close to 1, and thus $g(r_0, \omega)$ has a magnitude much larger than 1. This means that the near-field self-interaction of a large-size Raman resonant molecule with its plasmonic environment can become very significant and cannot be neglected, which is just the situation in the UHV-TERS Raman mapping experiment in ref 11. In such a situation, the traditional SERS and TERS theory as described in eq 3.1 is no longer accurate and must be subject to a significant modification as described in eq 4.23.

Further notes can be made for the usual SERS and TERS experiments involving small molecules such as Rhodamine 6G (Rh6G). These small molecules have a size far below one nanometer and a very small polarizability in the order of 1 atom unit, i.e., 1.65×10^{-41} C·m^2/V. In a usual TERS setup, the nanogap width is 1 order of magnitude larger than the molecule size. As a result, the near-field self-interaction term $\beta(\omega)\overleftrightarrow{\mathbf{G}}(r_0, r_0, \omega)$ has a magnitude far below 1, and thus, $g(r_0, \omega)$ has a magnitude close to 1. This means that the self-interaction of a usual small molecule with its plasmonic environment is very small and can be neglected. In these situations, the traditional SERS and TERS theory hold with high accuracy.

Because of the strong self-interaction of molecule with its environment of plasmonic resonant nanocavity, the modification factor is very sensitive to the overall geometric configuration and physical constitution of the strongly coupled nanosystem of metal nanogap and molecule. One significant thing is that the molecule itself is an indispensible part of the coupled system, therefore, any change to the molecule should change the property of the coupled system. This change should include the spatial location shift of molecule relative to the metal nanogap along both the horizontal and vertical directions in the geometric configuration. This geometric change will induce significant change to the Raman scattering intensity of molecule, and this is the physical origin of ultrahigh sensitivity of Raman signal to the TERS tip scanning position and the corresponding subnanometer spatial resolution in Raman mapping. This conclusion can also be made based on a more mathematical argument. Note that when the near-field self-interaction term $\beta(\omega)\overleftrightarrow{\mathbf{G}}(r_0, r_0, \omega)$ is close to 1 in magnitude, the modification factor $g(r_0, \omega)$ can be highly nonlinear with respect to the molecule position r_0, leading to ultrahigh sensitivity of Raman signal upon the relative position of molecule to the metal nanogap, namely the Ag tip.

The above theoretical analysis is largely qualitative. The next step is to estimate quantitatively to what extent the physical mechanism of significant near-field self-interaction can enhance the sensitivity and spatial resolution of Raman mapping by using UHV-TERS setup. The first important parameter that needs to establish is the molecule polarizability. Here the Clausius–Mossotti relation[30] is used to estimate the parameter. Assume that the molecules form a macroscopic perfect, homogeneous and isotropic dielectric with the constant about $\varepsilon = 3$, and the average volume of one molecule is about the value of a sphere of radius $r_m = 1$ nm due to its big atomic number. Then the polarizability of single molecule is about $\beta(\omega) = 4\pi\varepsilon_0(\varepsilon - 1)/(\varepsilon + 2)r_m^3 = 0.45 \times 10^{-37}$ C·m^2/V). Yet, the precise value of this molecular polarizability depends on several factors, such as the excitation wavelength and the orientation angle of the molecule skeleton. The second important parameter is the lateral and longitudinal position of the molecule relative to the TERS tip, denoted as x_0 and d_1. After these parameters are established, the near-field self-interaction modified Raman signal as a function of the molecule lateral displacement with respect to the Ag tip can be calculated to reveal the spatial resolution of Raman mapping.

The calculation for the Raman signal from the hybrid system including the Ag tip–substrate nanogap and molecule starts from determination of the unmodified local field profile by using the 3D FDTD method, which has been displayed in Figure 1. Then the unmodified and modified Raman scattering theory are adopted to calculate the Raman signal without and with consideration the near-field self-interaction of molecule with its plasmonic environment, respectively. A typical result is displayed in Figure 4 for $\beta = 0.45 \times 10^{-37}$ C·m^2/V) and d_1 =

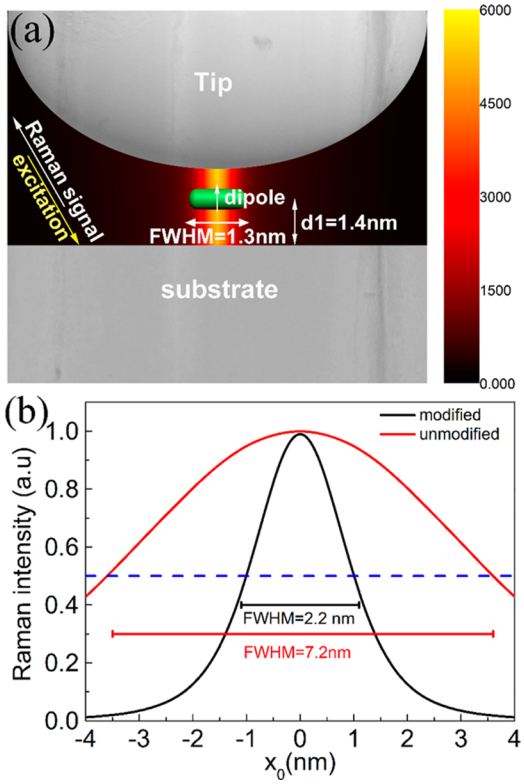

Figure 4. Local field profile and Raman signal when considering the electromagnetic self-interaction of molecule with the tip and substrate. (a) Calculated intensity profile of local field confined within the gap involving the molecule in self-interaction via multiple elastic scattering with the Ag tip–substrate gap. The molecular polarizability is $\beta = 0.45 \times 10^{-37}$ C·m^2/V), the lateral and longitudinal displacement of molecule to substrate are $x_0 = 0$ nm and $d_1 = 1.4$ nm. The fwhm of the "hot spot" is about 1.3 nm. (b) Raman signal intensity versus the lateral displacement of molecule x_0, as predicted by the unmodified (red) and modified (black) theory. The fwhm of the Raman signal is 7.2 and 2.2 nm for the unmodified and modified theory, respectively.

1.4 nm. Figure 4a clearly shows that the strong self-interaction would significantly reduce the "hot spot" size to about 1.3 nm, 1 order of magnitude smaller than the value without self-interaction (11 nm). As a result, the resolution of Raman mapping, which is assumed to equal the fwhm of the Raman response curve, can reach 2.2 nm, more than 3 times smaller than the unmodified value of 7.2 nm.

The above result has indicated the formation of "super-hot spot" due to strong coupling of the molecule with the tip–

DOI: 10.1021/acs.jpcc.5b02653
J. Phys. Chem. C 2015, 119, 11858–11871

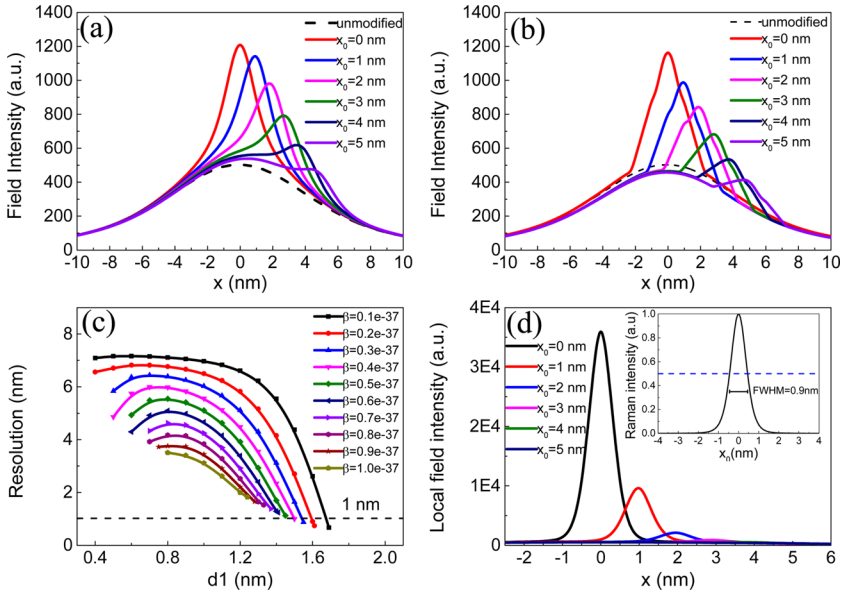

Figure 5. "Super-hot spot" formation and ultrahigh resolution in Raman mapping. (a) Local field intensity versus the horizontal coordinate-x as calculated by modified theory and 3D FDTD method for different lateral displacement of molecule (the molecular polarizability is $\beta = 0.45 \times 10^{-37}$ C·m^2/V), the lateral and longitudinal displacement of molecule to substrate are $x_0 = 0$ nm and $d_1 = 1.0$ nm). The dashed black curve represents the unmodified local field calculated by 3D FDTD method. (b) Local field intensity versus the horizontal coordinate-x as calculated by 3D FDTD method for different lateral displacement of molecule (the molecule is modeled by a dielectric sphere with radius 1 nm, relative dielectric constant 3, the lateral and longitudinal displacement of sphere to substrate are $x_0 = 0$ nm and $d_1 = 1.0$ nm). (c) Raman mapping resolution at different values of the longitudinal displacement of molecule to the substrate d_1 and molecular polarizability β. (d) Local field intensity versus the lateral displacement of molecule at $\beta = 0.2 \times 10^{-37}$ C·m^2/V and $d_1 = 1.6$ nm. The insert figure is the corresponding Raman intensity versus the lateral displacement, showing the fwhm of Raman signal (equal to the resolution) of 0.9 nm.

substrate nanogap and this "super-hot spot" is responsible for the much improved Raman mapping resolution. On the other hand, the property of the "super-hot spot" could be dependent on the relative position (longitudinal and lateral) of the molecule with respect to the tip apex. This feature is investigated in details by using the modified self-interaction theory. The result of local field intensity profile at each value of molecule lateral displacement, i.e., x_0, is displayed in Figure 5a. The molecule is excited at 532 nm and located at $d_1 = 1$ nm. To confirm the accuracy of the theoretical result, the 3D FDTD method is also used to reexamine the problem by modeling the molecule as a dielectric sphere with radius 1 nm and relative dielectric constant 3. The numerical result is displayed in Figure 5b, which agrees well with the theoretical result in regard to the line-shape of the curve and the peak intensity and position. For the sake of comparison, the unmodified local field intensity profile without considering self-interaction is also plotted in Figure 5, parts a and b. At $x_0 = 0$, the "super-hot spot" has the greatest enhancement and narrowest line width. When x_0 increases, the self-interaction induced field profile curve gets lower and wider, as a result of which the Raman mapping resolution does not obey the relation predicted by the conventional theory that the Raman mapping resolution is about half the "super-hot spot" size. Such a situation has already been illustrated in Figure 3.

A systematic exploration on the key issue of Raman mapping resolution is made in a broad space of parameters β and d_1 by using the trusty self-interaction modified theory, and the calculation results are summarized in Figure 5c. A significant point is that in some certain parameter space where the molecule is closer to the tip than to the substrate, the Raman mapping resolution could be below 1 nm. A typical example is illustrated in Figure 5d, where the "super-hot spot" field intensity profile at various values of the lateral displacement of molecule are displayed. Here the molecule polarizability is at a modest value of $\beta = 0.2 \times 10^{-37}$ C·m^2/V and located at the position of $d_1 = 1.6$ nm. Note that this molecule polarizability is substantially smaller than the value estimated for a sphere 1 nm at radius, $\beta = 0.45 \times 10^{-37}$ C·m^2/V, and is closer to the value of flat H2TBBP molecule which has a horizontal scale of ~2 nm and vertical scale of below 1 nm. At $x_0 = 0$, the "super-hot spot" has the greatest enhancement factor in peak intensity of 3600 and the narrowest line width of 0.8 nm, which are 72 times larger and 13 times smaller respectively than the corresponding values for the bare "hot spot" in Figure 1 without considering molecule self-interaction. Remarkably, the peak intensity of the "super-hot spot" rapidly decays down to about $^1/_4$ when x_0 increases to 1 nm. The decay is much more violent than the situation at Figure 5, parts a and b, which indicates that the Raman signal could be highly sensitive to the molecule lateral displacement leading to an ultrahigh spatial resolution in Raman mapping. Subsequent calculation based on the self-interaction modified theory is made and the result is displayed in the inset of Figure 5d. The Raman signal response curve has a fwhm of 0.9 nm, which implies a 0.9 nm resolution in Raman mapping, justifying the above expectation. Further calculation shows that this resolution is fine enough to discriminate two identical molecules 1 nm in lateral distance by Raman mapping (Figure 6).

VI. ESTIMATE OF NEAR-FIELD SELF-INTERACTION CONTRIBUTION TO RAMAN ENHANCEMENT

In the last few sections, we have developed a new optical theory of Raman scattering of molecules interacting not only with the incident light, which is subject to great enhancement in both Raman excitation and radiation strengths, but also with its

DOI: 10.1021/acs.jpcc.5b02653
J. Phys. Chem. C 2015, 119, 11858−11871

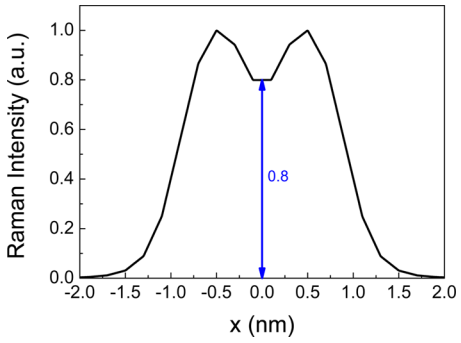

Figure 6. Raman mapping of two molecules in the TERS system. Calculated Raman intensity versus the horizontal coordinate-x for two identical molecules in lateral distance of 1 nm. Both molecules have polarizability $\beta = 0.2 \times 10^{-37}$ C·m^2/V) and they are located $d_1 = 1.6$ nm above the Ag substrate. The result is calculated by the modified theory considering molecule self-interaction. The two molecules are discernible by the Raman mapping.

complex near-field self-interaction with the plasmonic nanostructure environment. According to our numerical simulations, the new theory applied to TERS system can well explain the experimental observation of subnanometer spatial resolution in Raman mapping. In this section we further present an analysis to estimate the near-field self-interaction contribution to Raman scattering, in order to better understand the new Raman scattering theory associated with various TERS systems under a broad range of geometric parameters and operational conditions.

The new theory involves contributions from two new modification factors $g_1(r_0, \omega)$ and $g_2(r_0, \omega_R)$, in addition to the factors described by the traditional Raman scattering theory. It is thus pivotal to make deep quantitative analyses on the roles played by these modification factors on our current problem of subnanometer resolution in the Raman mapping using TERS, among which their magnitude and spatial sensitivity needs special attention.

Let us take a closer look at the near-field self-interaction modification-factor tensor $\overleftrightarrow{\mathbf{g}}_1(r_0, \omega) = [\overleftrightarrow{\mathbf{I}} - \beta(\omega)(\omega^2/\varepsilon_0 c^2) \sum_i \overleftrightarrow{\mathbf{G}}_0(r_0, r_i, \omega)\overleftrightarrow{\mathbf{M}}_i]^{-1}$. Let $k_0 = \omega/c$ be the free-space wavenumber, the free−space Green function $\overleftrightarrow{\mathbf{G}}_0(r_0, r_i, \omega)$ is given by

$$
\begin{aligned}
\overleftrightarrow{\mathbf{G}}_0(\mathbf{r}_0, \mathbf{r}_i, \omega) &= \left(\frac{1}{k_0^2}\nabla\nabla + \overleftrightarrow{\mathbf{I}}\right) G_0(\mathbf{r}_0, \mathbf{r}_i, \omega) = \frac{1}{4\pi}\left(\frac{1}{k_0^2}\nabla\nabla + \overleftrightarrow{\mathbf{I}}\right)\frac{e^{ik_0|\mathbf{r}_0-\mathbf{r}_i|}}{|\mathbf{r}_0-\mathbf{r}_i|} \\
&= \frac{1}{4\pi}\begin{pmatrix} \frac{1}{k_0^2}\frac{\partial^2}{\partial x^2} + 1 & \frac{1}{k_0^2}\frac{\partial}{\partial x}\frac{\partial}{\partial y} & \frac{1}{k_0^2}\frac{\partial}{\partial x}\frac{\partial}{\partial z} \\ \frac{1}{k_0^2}\frac{\partial}{\partial y}\frac{\partial}{\partial x} & \frac{1}{k_0^2}\frac{\partial^2}{\partial y^2} + 1 & \frac{1}{k_0^2}\frac{\partial}{\partial y}\frac{\partial}{\partial z} \\ \frac{1}{k_0^2}\frac{\partial}{\partial z}\frac{\partial}{\partial x} & \frac{1}{k_0^2}\frac{\partial}{\partial z}\frac{\partial}{\partial y} & \frac{1}{k_0^2}\frac{\partial^2}{\partial z^2} + 1 \end{pmatrix}\frac{e^{ik_0|\mathbf{r}_0-\mathbf{r}_i|}}{|\mathbf{r}_0-\mathbf{r}_i|} \\
&\approx \frac{1}{4\pi k_0^2}\begin{pmatrix} \frac{3(x_0-x_i)^2}{|\mathbf{r}_0-\mathbf{r}_i|^2} - 1 & \frac{3(x_0-x_i)(y_0-y_i)}{|\mathbf{r}_0-\mathbf{r}_i|^2} & \frac{3(x_0-x_i)(z_0-z_i)}{|\mathbf{r}_0-\mathbf{r}_i|^2} \\ \frac{3(y_0-y_i)(x_0-x_i)}{|\mathbf{r}_0-\mathbf{r}_i|^2} & \frac{3(y_0-y_i)^2}{|\mathbf{r}_0-\mathbf{r}_i|^2} - 1 & \frac{3(y_0-y_i)(z_0-z_i)}{|\mathbf{r}_0-\mathbf{r}_i|^2} \\ \frac{3(z_0-z_i)(x_0-x_i)}{|\mathbf{r}_0-\mathbf{r}_i|^2} & \frac{3(z_0-x_i)(z_0-y_i)}{|\mathbf{r}_0-\mathbf{r}_i|^2} & \frac{3(z_0-z_i)^2}{|\mathbf{r}_0-\mathbf{r}_i|^2} - 1 \end{pmatrix}\frac{e^{ik_0|\mathbf{r}_0-\mathbf{r}_i|}}{|\mathbf{r}_0-\mathbf{r}_i|^3} \\
&= \frac{1}{4\pi k_0^2}\frac{e^{ik_0|\mathbf{r}_0-\mathbf{r}_i|}}{|\mathbf{r}_0-\mathbf{r}_i|^3}\overleftrightarrow{\mathbf{B}}_i
\end{aligned}
\tag{6.1}
$$

Here in deriving the final equation of eq 6.1, we have adopted the quasi-static approximation based on the fact that in the deep-subwavelength near-field region, this model works very well. The matrix $\overleftrightarrow{\mathbf{B}}_i$ reflects the orientation of near-field dipole radiation, and its magnitude is in the order of the unit matrix $\overleftrightarrow{\mathbf{I}}$. We can see that in the deep-subwavelength near-field region, the free−space Green function is inversely proportional to cubic power of the dipole-image dipole distance $|r_0 - r_i|$.

Now let us look at the matrix $\overleftrightarrow{\mathbf{M}}_i$, which is a tensor describing the self-interaction of the molecule dipole with either the lower-side flat Ag substrate or the upper-side Ag curved tip modeled by a Ag sphere. In the deep-subwavelength near-field region, this self-interaction effect can be approximated with high accuracy by interaction of the dipole with an image dipole located either within the substrate or within the spherical tip. As a result, $\overleftrightarrow{\mathbf{M}}_i$ are called image matrix. According to refs 32 and 33, we can get the explicit analytical form of this image matrix. The recursion relation for the image matrix relative to the lower-side flat substrate is $\overleftrightarrow{\mathbf{M}}_i = ((\varepsilon_m - 1)/(\varepsilon_m + 1))(-n_x n_x - n_y n_y + n_z n_z)\overleftrightarrow{\mathbf{M}}_{i-1}$, with n_x, n_y, and n_z being the three unit vectors in the Cartesian coordinates relative to the metal substrate. Similarly, the image matrix relative to the upper-side metal sphere has a recursion relation as $\overleftrightarrow{\mathbf{M}}_i = ((\varepsilon_m - 1)/(\varepsilon_m + 1))(-n_\theta n_\theta - n_\varphi n_\varphi + n_r n_r)\overleftrightarrow{\mathbf{M}}_{i-1}$ by referring to the semi-infinite dielectric and the conducting sphere. n_θ, n_φ, and n_r are the three unit vectors in the spherical coordinates relative to the metal

DOI: 10.1021/acs.jpcc.5b02653
J. Phys. Chem. C 2015, 119, 11858−11871

sphere. In wave optics, the image matrices just represent the reflection of dipole radiation from the flat Ag substrate and curved Ag sphere. As we have seen in section II, these radiation fields are subject to multiple reflection within the gap by the lower and upper Ag-air interfaces, leading to the existence of a series of image dipoles and image matrices. Although the magnitude of each image matrix $\overleftrightarrow{\mathbf{M}}_i$ is in the order of unit matrix $\overleftrightarrow{\mathbf{I}}$, all these image matrices that represent the interaction among these image dipoles could sum up to a significant magnitude, and in some special situations could trigger resonance interaction of the molecule dipole with its plasmonic environment, namely the lower and upper Ag substrates.

The final factor is the molecular polarizability, $\beta(\omega)$, which relates the molecule dipole moment $\boldsymbol{p}$ with the excitation electric field by $\boldsymbol{p} = \beta(\omega)\boldsymbol{E}$. Basically, this factor is proportional to the volume of the molecule V_m in the macroscopic aspect and the dipole transition probability denoted as $\boldsymbol{d}_{\mathrm{m}}$ (usually with a magnitude in the order of 1, unless at condition of Raman resonance) between lower and upper molecule quantum states in the microscopic aspect. The molecule volume V_m is related with its linear size r_m via $V_m = 4\pi r_m^3/3$. Therefore, $\beta(\omega) \approx 4\pi\varepsilon_0 r_m^3 d_m/3$.

Now the near-field self-interaction modification-factor tensor is approximately written as

$$\overleftrightarrow{\mathbf{g}}_1(\mathbf{r}_0, \omega) = \left[\overleftrightarrow{\mathbf{I}} - \frac{d_m}{3}\sum_i \frac{r_m{}^3 \mathrm{e}^{ik_0|\mathbf{r}_0 - \mathbf{r}_i|}}{|\mathbf{r}_0 - \mathbf{r}_i|^3}\overleftrightarrow{\mathbf{B}}_i\overleftrightarrow{\mathbf{M}}_i\right]^{-1} \tag{6.2}$$

Equation 6.2 tells us many things. Note that for a usual small molecule, the size is below one nanometer, and the polarizability is always very small and is in the order of au = 1.648777×10^{-41} C·m^2/V). When this molecule is placed close to usual plasmonic nanostructures, the distance of the molecule to the surface is in the order of several nanometers or more, 1 order of magnitude larger than the molecule linear size. Besides, the molecule radiation interacts with the plasmonic nanostructure only once. As a result, the term $(d_m/3)\sum_i((r_m{}^3\mathrm{e}^{ik_0|r_0 - r_i|})/(|r_0 - r_i|^3))\overleftrightarrow{\mathbf{B}}_i\overleftrightarrow{\mathbf{M}}_i$ has a magnitude far below 1, and thus $\overleftrightarrow{\mathbf{g}}_1(r_0, \omega)$ has a magnitude close to 1. This means that the self-interaction of a usual small molecule with its plasmonic environment is very small and can be neglected. In these situations, the traditional SERS and TERS theory hold with high accuracy.

It can also be clear from eq 6.2 what can be done to greatly enhance the molecule near-field self-interaction modification factor, $g_1(r_0, \omega) \approx (1/3)\mathrm{Tr}[\overleftrightarrow{\mathbf{g}}_1(r_0, \omega)]$. Several schemes can be adopted to achieve this. First, increase the molecule size r_m and make the molecule very close to the metal surface so that r_m is comparable with the dipole-image dipole distance $|r_0 - r_i|$. Second, increase the molecule dipole transition probability $\boldsymbol{d}_{\mathrm{m}}$, for instance by adopting the condition of Raman resonance. Third, increase the number of image dipoles with non-negligible contribution, for instance by adopting a plasmonic resonant cavity nanostructure with efficient multiple reflection effects, so as to make the overall self-interaction much larger than a single dipole-image dipole interaction.

When all the enhancement schemes are involved within a single system, their contributions can be summed up to a large magnitude. This is just the situation in the current UHV-TERS Raman mapping experiment by Dong and co-workers,[11] in which the H2TBPP organic molecule has a linear size in the order of 1−2 nm, it is placed within the Ag-substrate Ag-tip nanogap so that its radiation is subject to an efficient multiple reflection effect. Besides, the gap is on the order of several nanometers, so that the molecule distances to the lower and upper surface are both on the order of 1−2 nm. In addition, the Raman radiation of molecule is excited under the resonance condition in which the excitation wavelength matches well with the direct Raman transition band instead of the usual transition assisted by virtual photons. Considering all these factors, the term $(d_m/3)\sum_i((r_m{}^3\mathrm{e}^{ik_0|r_0 - r_i|})/(|r_0 - r_i|^3))\overleftrightarrow{\mathbf{B}}_i\overleftrightarrow{\mathbf{M}}_i$ can have a magnitude close to 1, and thus $\overleftrightarrow{\mathbf{g}}_1(r_0, \omega)$ has a magnitude much larger than 1. This means that the near-field self-interaction of a large-size Raman resonant molecule with its plasmonic environment can be significant and cannot be neglected. In the situation, the traditional SERS and TERS theory is no longer accurate and must be subject to a significant modification. Yet, the precise quantitative value of this near-field self-interaction modification factor must be determined numerically.

Because of the strong self-interaction of molecule with its environment of plasmonic resonant nanocavity, the modification factor should be very sensitive to the overall geometric configuration and physical constitution of the strongly coupled system of metal nanogap and molecule. One significant thing is that the molecule itself is an indispensible part of the coupled system, therefore, any change to the molecule should change the property of the coupled system. This change should include the spatial location shift of molecule relative to the metal nanogap along both the horizontal and vertical directions in the geometric configuration. This geometric change will induce a significant change to the Raman scattering intensity of molecule, and that is the physical origin of ultrahigh sensitivity of Raman signal to the TERS tip scanning position and the corresponding subnanometer spatial resolution in Raman mapping. This conclusion can also be made based upon a more mathematical argument. Note that when the term $(d_m/3)\sum_i((r_m{}^3\mathrm{e}^{ik_0|r_0 - r_i|})/(|r_0 - r_i|^3))\overleftrightarrow{\mathbf{B}}_i\overleftrightarrow{\mathbf{M}}_i$ is close to 1 in magnitude, the modification factor $\overleftrightarrow{\mathbf{g}}_1(r_0, \omega)$ and its magnitude $g_1(r_0, \omega) \approx (1/3)\mathrm{Tr}[\overleftrightarrow{\mathbf{g}}_1(r_0, \omega)]$ can be highly nonlinear with respect to the molecule position r_0. And this leads to ultrahigh sensitivity of Raman signal upon the relative position of molecule to the metal nanogap, namely the Ag tip.

Now we can use this general physical picture to understand the UHV-TERS system that we study in this work. The Ag tip has a small curvature radius as 25 nm, thus when the tip is displaced away from the center of the H2TBPP organic molecule along the horizontal direction, the vertical distance of the tip to the center of the molecule is increased, leading to an increase in the distance between the molecular dipole with its image dipoles inside the Ag tip and thus a significant reduction in their interaction strengths as well as the magnitude of the self-interaction modification factor $g_1(r_0, \omega)$. This means that the Raman signal would reach the maximum value when the Ag tip is right at the top of the molecular center, and rapidly reduces when the tip is displaced in the lateral direction from the molecular center. As a result, the spatial resolution of Raman mapping is much finer than the hot spot of nanogap mode can support. Besides, notice that this reduction of self-interaction strength would become more violent when the molecule is vertically closer to the tip, because now the molecule would sense a more curved surface of the tip and its interaction with the image dipoles would change much rapidly when the tip is laterally displaced. Therefore, the spatial resolution of Raman mapping is increased in this situation. All these qualitative arguments overall agree well with our

DOI: 10.1021/acs.jpcc.5b02653
J. Phys. Chem. C 2015, 119, 11858−11871

quantitative numerical calculations as discussed in Figures 4 and 5.

In the history of SERS, some authors have considered the classic electromagnetic or quantum interaction between molecule and metal nanostructures by using the similar dipole-image dipole interaction model as our new Raman theory.[1,31,36,37] It was found that the modification for Raman signal was tiny and negligible for a molecule above a flat metal surface. We note that this observation is consistent with our theoretical model. As the dipole and its image dipole only interact once, the overall interaction strength is very small. Only multiple interactions can sum up to induce considerable modification effect. As a result, in some special plasmonic nanostructures such as the current nanogap, this self-interaction induced modification to Raman signal in both spectral and spatial dependence must be accounted for. However, in many other plasmonic nanostructures, such as those with an open geometry, such a modification effect might be small and can be neglected.

The final issue is about the validity of using classical electrodynamics to handle the molecule interaction with the plasmonic nanogap. We note that the dipole-image dipole interaction model has long been popularly adopted in classical electrodynamics and optics and it is indeed a good approximation in describing molecular dipole radiation influenced by a metal surface if the molecule is not directly sitting on the surface, but has a distance so that the classical electrodynamics model, in particular, assuming a sharp interface between vacuum and metal surface can be applicable. This distance could be as small as 0.3 nm (a size of several Ag atom lattices). Beyond this distance, the quantum plasmonic effect considering specific electronic structure of conduction electrons in metal surface can be neglected.[38,39] In the TERS system under study, the gap between Ag tip and Ag flat substrate is 2 nm, the molecule is in the middle of the gap, and the distance of molecule with respect to the tip and substrate is beyond the range that quantum plasmonics effect can play a key role.[38,39] Thus, the methodology of classical electrodynamics can be well applicable.

VII. CONCLUSION AND PERSPECTIVE

In summary, we have presented an optical theory of Raman scattering to account for the spatial resolution of Raman mapping against a molecule placed within a plasmonic nanogap in a UHV-TERS system. This theory has fully considered the near-field self-interaction of molecule with the plasmonic nanogap in both the Raman excitation and radiation processes. We have found that the strong plasmonic resonance effect in the plamsonic nanogap would induce multiple elastic scattering of the molecule upon the optical field of the gap mode. Because the molecule has a size comparable with the nanogap distance, this self-interaction effect can strongly modulates the Raman excitation and radiation in both the signal intensity and spatial sensitivity. The self-interaction strength can be large enough to create a "super-hot spot" with a size on the order of nanometer within the plasmonic nanogap. Besides, due to the self-interaction, the molecule-nanogap has become a strongly correlated nanosystem that involves an ultrastrong correlation of Raman signal with the molecule-nanogap physical and geometric configuration, where the molecule polarizability and its lateral and longitudinal position are all key contributing elements. This ultrastrong correlation between the Raman signal intensity and the lateral position of molecule relative to the tip has a direct consequence of ultrahigh lateral spatial resolution of Raman mapping that is much finer than the "hot-spot" size of the passive nanogap plasmonic mode. In short, the subnanometer ultrahigh Raman mapping resolution observed in ref11 can be attributed to the strong optical coupling of the molecule with its plasmonic nanogap environment via multiple elastic scattering. An optical theory of Raman scattering can well explain the experimental observation, much the same as the conventional optical theory of SERS can well explain and predict Raman signal enhancement in numerous plasmonic nanostructures.

Besides offering a good explanation on the experimental data, our theoretical studies also raise some issues that are worth mentioning. First, the highly sensitive Raman signal to the molecule lateral and vertical position means that ultrahigh stable molecule positioning is requested and thus UHV-TERS system is necessary for reliable Raman mapping. Otherwise, any displacement motion of molecule, e.g., thermal fluctuation would make the Raman spectral imaging and mapping unstable and unreliable. Second, the self-interaction optical theory not only well explains the physical origin of subnanometer ultrahigh Raman mapping resolution, but also reveals a new understanding of electromagnetic Raman enhancement mechanism. In conventional Raman theory, the SPR induced local field enhancement is the most important channel to enhance Raman signal optically. Now, the self-interaction of molecule with its plasmonic environment offers another major channel to enhance Raman signal optically at the gap plasmons mode with nanometer gap sizes. In Figure 1a, the normal theory predicts a Raman enhancement factor of about 10^4-10^5; however, in Figure 5d, the self-interaction greatly increases the enhancement factor to about 10^7-10^8. Obviously, this new mechanism can be further explored in a plenty of SERS substrates with an already sufficiently high enhancement factor ($10^{10}-10^{12}$)[40,41] for further pushing the upper detection limit to the single molecule level ($10^{14}-10^{15}$).[4,5,20] Finally, our theory and the associated physical picture of Raman scattering might also suggest a possible routine to further enhance the spatial resolution of Raman mapping by optimizing the geometrical configurations and operational conditions of UHV-TERS.

The new optical theory of Raman scattering constitutes a good example showing how important it is to consider near-field self-interaction of molecules with plasmonic nanostructures for drawing a complete and accurate physics picture of nanoscale light-matter interaction both at the classical physics and quantum physics level. The concept and methodology of the theory can be straightforwardly extended to handle other optical physical processes and could be helpful to have a deeper understanding to a variety of phenomena such as SERS, fluorescence enhancement and ultrahigh sensitivity biosensors. The existence of "super-hot spot" originating from this near-field self-interaction can make Raman and fluorescence signals stronger and biosensor more sensitive than usually expected, and help explore more powerful nanophotonic imaging, emitting, and sensing technologies. We expect that the new theory and the associated principle can become very helpful for uncovering the full picture of light-matter interaction of atoms and molecules with plasmonic nanostructures and explore unknown frontiers of physics and chemistry at nanoscale.

DOI: 10.1021/acs.jpcc.5b02653
J. Phys. Chem. C 2015, 119, 11858−11871

AUTHOR INFORMATION

Corresponding Author

*(Z.-Y.L.) E-mail: lizy@aphy.iphy.ac.cn.

Notes

The authors declare no competing financial interest.

ACKNOWLEDGMENTS

This work is supported by the 973 Program of China at No. 2013CB632704 and 2011CB922002, and the National Natural Science Foundation of China at No. 11374357. The authors thank Prof. Zhen-Chao Dong from the University of Science and Technology of China for stimulating discussions.

REFERENCES

(1) Moskovits, M. Surface-Enhanced Spectroscopy. *Rev. Mod. Phys.* **1985**, *57*, 783−826.

(2) Otto, A.; Mrozek, I.; Grabhorn, H.; Akemann, W. J. Surface-Enhanced Raman Scattering. *J. Phys.: Condens. Matter* **1992**, *4*, 1143−1212.

(3) Campion, A.; Kambhampati, P. Surface-Enhanced Raman Scattering. *Chem. Soc. Rev.* **1998**, *27*, 241−250.

(4) Kneipp, K.; Wang, Y.; Kneipp, H.; Perelman, L. T.; Itzkan, I.; Dasari, R. R.; Feld, M. S. Single Molecule Detection Using Surface-Enhanced Raman Scattering (SERS). *Phys. Rev. Lett.* **1997**, *78*, 1667−1670.

(5) Nie, S.; Emory, S. R. Probing Single Molecules and Single Nanoparticles by Surface-Enhanced Raman Scattering. *Science* **1997**, *275*, 1102−1106.

(6) Anderson, M. S. Locally Enhanced Raman Spectroscopy with an Atomic Force Microscope. *Appl. Phys. Lett.* **2000**, *76*, 3130−3132.

(7) Hartschuh, A.; Sánchez, E. J.; Xie, X. S.; Novotny, L. High-Resolution Near-Field Raman Microscopy of Single-Walled Carbon Nanotubes. *Phys. Rev. Lett.* **2003**, *90*, 095503.

(8) Steidtner, J.; Pettinger, B. Tip-Enhanced Raman Spectroscopy and Microscopy on Single Dye Molecules with 15 nm Resolution. *Phys. Rev. Lett.* **2008**, *100*, 236101.

(9) Yano, T.; Verma, P.; Saito, Y.; Ichimura, T.; Kawata, S. Pressure-Assisted Tip-Enhanced Raman Imaging at a Resolution of a Few Nanometers. *Nat. Photonics* **2009**, *3*, 473−477.

(10) Jiang, N.; Foley, E. T.; Klingsporn, J. M.; Sonntag, M. D.; Valley, N. A.; Dieringer, J. A.; Seideman, T.; Schatz, G. C.; Hersam, M. C.; Van Duyne, R. P. Observation of Multiple Vibrational Modes in Ultrahigh Vacuum Tip-Enhanced Raman Spectroscopy Combined with Molecular-Resolution Scanning Tunneling Microscopy. *Nano Lett.* **2012**, *12*, 5061−5067.

(11) Zhang, R.; Zhang, Y.; Dong, Z. C.; Jiang, S.; Zhang, C.; Chen, L. G.; Zhang, L.; Liao, Y.; Aizpurua, J.; Luo, Y.; et al. Chemical Mapping of a Single Molecule by Plasmon-Enhanced Raman Scattering. *Nature* **2013**, *498*, 82−86.

(12) Novotny, L.; Bert, H. *Principles of Nano-Optics*. Cambridge University Press: Cambridge, U.K., 2012.

(13) Ichimura, T.; Hayazawa, N.; Hashimoto, M.; Inouye, Y.; Kawata, S. Tip-Enhanced Coherent Anti-Stokes Raman Scattering for Vibrational Nanoimaging. *Phys. Rev. Lett.* **2004**, *92*, 220801.

(14) Ichimura, T.; Watanabe, H.; Morita, Y.; Verma, P.; Kawata, S.; Inouye, Y. Temporal Fluctuation of Tip-Enhanced Raman Spectra of Adenine Molecules. *J. Phys. Chem. C* **2007**, *111*, 9460−9464.

(15) Sun, M.; Zhang, Z. L.; Zheng, H. R.; Xu, H. X. In-Situ Plasmon-Driven Chemical Reactions Revealed by High Vacuum Tip-Enhanced Raman Spectroscopy. *Sci. Rep.* **2012**, *2*, 647.

(16) Anger, P.; Bharadwaj, P.; Novotny, L. Enhancement and Quenching of Single-Molecule Fluorescence. *Phys. Rev. Lett.* **2006**, *96*, 113002.

(17) Kinkhabwala1, A.; Yu, Z.; Fan, S.; Avlasevich, Y.; Müllen, K.; Moerner, W. E. Large Single-Molecule Fluorescence Enhancements Produced by a Bowtie Nanoantenna. *Nat. Photonics* **2009**, *3*, 654−657.

(18) Noginov, M. A.; Zhu, G.; Belgrave, A. M.; Bakker, R.; Shalaev, V. M.; Narimanov, E. E.; Tout, S.; Herz, E.; Suteewong, T.; Wiesner, U. Demonstration of a Spaser-Based Nanolaser. *Nature* **2009**, *460*, 1110−1112.

(19) Liu, S.; Huang, L.; Li, J. F.; Wang, C.; Li, Q.; Xu, H. X.; Guo, H. L.; Meng, Z. M.; Shi, Z.; Li, Z. Y. Simultaneous Excitation and Emission Enhancement of Fluorescence Assisted by Double Plasmon Modes of Gold Nanorods. *J. Phys. Chem. C* **2013**, *117*, 10636−10642.

(20) Li, Z. Y.; Xia, Y. N. Metal Nanoparticles with Gain toward Single-Molecule Detection by Surface-Enhanced Raman Scattering. *Nano Lett.* **2010**, *10*, 243−249.

(21) Huang, X. Q.; Tang, S. H.; Mu, X. L.; Dai, Y.; Chen, G. X.; Zhou, Z. Y.; Ruan, F. X.; Yang, Z. L.; Zheng, N. F. Freestanding Palladium Nanosheets with Plasmonic and Catalytic Properties. *Nat. Nanotechnol.* **2011**, *6*, 28−32.

(22) Christopher, P.; Xin, H. L.; Linic, S. Visible-Light-Enhanced Catalytic Oxidation Reactions on Plasmonic Silver Nanostructures. *Nat. Chem.* **2011**, *3*, 467−472.

(23) Zhong, X. L.; Li, Z. Y. Giant Enhancement of Near-Ultraviolet Light Absorption by TiO_2 via a Three-Dimensional Aluminum Plasmonic Nano Funnel-Antenna. *J. Phys. Chem. C* **2012**, *116*, 21547−21555.

(24) Kauranen, M.; Zayats, A. V. Nonlinear Plasmonics. *Nat. Photonics* **2012**, *6*, 737−748.

(25) Knight, M. W.; Sobhani, H.; Nordlandera, P.; Halas, N. J. Photodetection with Active Optical Antennas. *Science* **2011**, *332*, 702−704.

(26) Brown, L. V.; Zhao, K.; King, N.; Sobhani, H.; Nordlander, P.; Halas, N. J. Surface-Enhanced Infrared Absorption Using Individual Cross Antennas Tailored to Chemical Moieties. *J. Am. Chem. Soc.* **2013**, *135*, 3688−3695.

(27) Schlathe, A. E.; Large, N.; Urban, A. S.; Nordlander, P.; Halas, N. J. Near-Field Mediated Plexcitonic Coupling and Giant Rabi Splitting in Individual Metallic Dimers. *Nano Lett.* **2013**, *13*, 3281−3286.

(28) Le Ru, E. C.; Etchegoin, P. G. Rigorous Justification of The $|E|^4$ Enhancement Factor in Surface Enhanced Raman Spectroscopy. *Chem. Phys. Lett.* **2006**, *423*, 63−66.

(29) Le Ru, E. C.; Blackie, E.; Meyer, M.; Etchegoin, P. G. Surface Enhanced Raman Scattering Enhancement Factors: a Comprehensive Study. *J. Phys. Chem. C* **2007**, *111*, 13794−13803.

(30) Jackson, J. D. *Classical Electrodynamics*. Wiley-VCH: Weinheim, Germany, 1998.

(31) Gersten, J.; Nitzan, A. Electromagnetic Theory of Enhanced Raman Scattering by Molecules Adsorbed on Rough Surfaces. *J. Chem. Phys.* **1980**, *73*, 3023−3037.

(32) Li, Z. Y.; Gu, B. Y.; Yang, G. Z. Modified Self-Consistent Approach Applied in Near-Field Optics for Mesoscopic Surface Defects. *Phys. Rev. B* **1997**, *55*, 10883−10894.

(33) Li, Z. Y.; Gu, B. Y.; Yang, G. Z. Scanning-electrostatic-force microscopy: Self-Consistent Method for Mesoscopic Surface Structures. *Phys. Rev. B* **1998**, *57*, 9225−9233.

(34) Ye, J.; Wen, F. F.; Sobhani, H.; Lassiter, J. B.; Van Dorpe, P.; Nordlander, P.; Halas, N. J. Plasmonic Nanoclusters: Near Field Properties of the Fano Resonance Interrogated with SERS. *Nano Lett.* **2012**, *12*, 1660−1667.

(35) Anker, J. N.; Hall1, W. P.; Lyandres, O.; Shah, N. C.; Zhao, J.; Van Duyne, P. R. Biosensing with Plasmonic Nanosensors. *Nat. Mater.* **2008**, *7*, 442−453.

(36) Johansson, P.; Xu, H.; Käll, M. Surface-Enhanced Raman Scattering and Fluorescence near Metal Nanoparticles. *Phys. Rev. B* **2005**, *72*, 035427.

(37) Kerker, M.; Wang, D. S.; Chew, H. Surface Enhanced Raman Scattering (SERS) by Molecules Adsorbed at Spherical Particles: Errata. *Appl. Opt.* **1980**, *19*, 4159−4174.

(38) Esteban, R.; Borisov, A. G.; Nordlander, P.; Aizpurua, J. Bridging Quantum and Classical Plasmonics with a Quantum-Corrected Model. *Nat. Commun.* **2012**, *3*, 825.

DOI: 10.1021/acs.jpcc.5b02653
J. Phys. Chem. C 2015, 119, 11858−11871

(39) Javier García de Abajo, F. Nonlocal Effects in the Plasmons of Strongly Interacting Nanoparticles, Dimers, and Waveguides. *J. Phys. Chem. C* **2008**, *112*, 17983−17987.
(40) Xu, H.; Bjerneld, E. J.; Käll, M.; Börjesson, L. Spectroscopy of Single Hemoglobin Molecules by Surface Enhanced Raman Scattering. *Phys. Rev. Lett.* **1999**, *83*, 4357−4360.
(41) Liu, Z.; Yang, Z. B.; Peng, B.; Cao, C.; Zhang, C.; Xiong, Q. H.; Li, Z. Y.; Fang, J. X. Highly Sensitive, Uniform, and Reproducible Surface-Enhanced Raman Spectroscopy from Hollow Au-Ag Alloy Nanourchins. *Adv. Mater.* **2014**, *26*, 2431−2439.

DOI: 10.1021/acs.jpcc.5b02653
J. Phys. Chem. C 2015, 119, 11858−11871